

Stochastic jetting and dripping in confined soft granular flows

Michał Bogdan,^{1,*} Andrea Montessori,² Adriano Tiribocchi,³ Fabio Bonaccorso,^{3,4}

Marco Lauricella,³ Leon Jurkiewicz,¹ Sauro Succi,^{3,5,6} and Jan Guzowski^{1,†}

¹*Institute of Physical Chemistry, Polish Academy of Sciences, Kasprzaka 44/52, 01-224 Warsaw, Poland*

²*Dipartimento di Ingegneria, Università degli Studi Roma tre, via Vito Volterra 62, Rome, 00146, Italy*

³*Istituto per le Applicazioni del Calcolo del Consiglio Nazionale delle Ricerche, via dei Taurini 19, 00185, Rome, Italy*

⁴*Department of Physics and National Institute for Nuclear Physics,*

University of Rome "Tor Vergata", Via Cracovia, 50, 00133 Rome, Italy

⁵*Center for Life Nanoscience at la Sapienza, Istituto Italiano di Tecnologia, viale Regina Elena 295, 00161, Rome, Italy*

⁶*Department of Physics, Harvard University, 17 Oxford St, Cambridge, MA 02138, United States*

(Dated: January 26, 2022)

We report new dynamical modes in confined soft granular flows, such as stochastic jetting and dripping, with no counterpart in continuum viscous fluids. The new modes emerge as a result of the propagation of the chaotic behaviour of individual grains- here, monodisperse emulsion droplets- to the level of the entire system as the emulsion is focused into a narrow orifice by an external viscous flow. We observe avalanching dynamics and the formation of remarkably stable jets- single-file granular chains- which occasionally break, resulting in a non-Gaussian distribution of cluster sizes. We find that the sequences of droplet rearrangements that lead to the formation of such chains resemble unfolding of cancer cell clusters in narrow capillaries, overall demonstrating that microfluidic emulsion systems could serve to model various aspects of soft granular flows, including also tissue dynamics at the meso-scale.

Soft granular materials consist of close-packed deformable grains separated by thin fluid films. They are ubiquitous in industries, forming food and cosmetic products and in nature, examples including dense emulsions, foams, as well as certain types of biological tissues, among others [1–7]. The presence of the internal lengthscale in such materials, associated with the grain size, leads to a complex many-body dynamics governed by the sequences of grain deformations and rearrangements [8, 9], which in turn result in complex flows and rheological behavior, including plasticity and viscoelasticity, memory effects and avalanches [10–15].

The flow of such types of materials confined to narrow geometries is of primary interest to the physics of amorphous solids and glasses [8, 9, 16], as well as of technological relevance for the generation of compartmentalized capsules [17] and porous materials [18] or in bioprinting [19]. The dynamics of soft granular media in constrictions under external flow is also of significant interest in tissue mechanics [20], as it could shed light on the behavior of cell clusters passing through physiological constrictions, a process that remains one of the critical stages of tumor metastasis.

Previous microfluidic approaches to soft granular materials addressed the behavior of foams or dense emulsions inside channels, however without considering the interaction with an external flow [8, 9, 13, 21, 22]. Here, we systematically study the behavior of a model 'wet' soft-granular medium (a tightly packed monodisperse emulsion) under external viscous forces. We use a flow-focusing geometry in which the emulsion is fed through

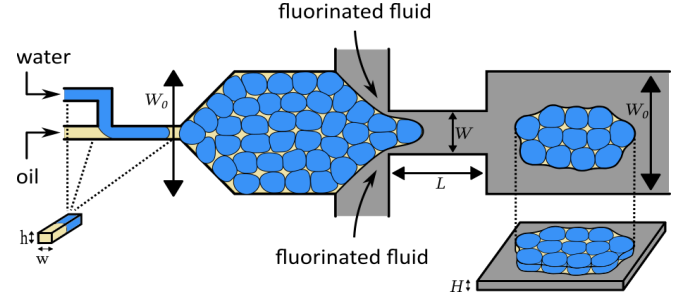


FIG. 1. Scheme of the microfluidic system for generation of a quasi-2D granular medium (water-in-oil emulsion) and its fragmentation under flow-focusing with an external third immiscible phase (fluorinated fluid). Dimensions as measured by profilometry are: $W_0 = 2$ mm, $W = 1$ mm, $L = 2$ mm, $H = 0.11$ mm, $w = 0.11$ mm, $h = 0.08$ mm.

the middle channel and the external immiscible phase through the side channels. Accordingly, the emulsion is focused by the external flow and narrows until passing through an orifice, a situation which closely resembles the flow of cell clusters in capillaries.

Typically, in microfluidics, flow-focusing junctions are used to generate highly monodisperse emulsions [23]. Thus, in Newtonian liquids, one typically observes two primary dynamical modes: dripping, in which monodisperse droplets are created inside the orifice, and jetting, in which the focused phase flows in parallel with the focusing phase beyond the orifice, only to break-up much later [23–25] due to the Rayleigh-Plateau instability [24], although other regimes have also been reported [23, 26, 27].

Here, in the case of a granular medium, we find new dynamical patterns, distinct from simple viscous jetting

* mbogdan@ichf.edu.pl

† jguzowski@ichf.edu.pl

and dripping, such as (i) formation of fluctuating jets in which the fluctuations of jet width are influenced by avalanche-like 'discharge' of the dispersed granular phase at the junction rather than by the Rayleigh-Plateau instability of the jet, (ii) formation of very thin jets- single-file chains of grains-via 'unfolding' of thicker jets under extensional viscous stresses, and (iii) irregular break-up of the jets resulting in highly polydisperse grain clusters with a non-Gaussian size distribution. We highlight the stochasticity of the transport of the close-packed emulsion through the orifice in the various regimes and the impact of the behavior of individual grains on the dynamics of the entire emulsion (e.g., its break-up). Furthermore, we perform ad-hoc numerical simulations based on a recently developed Lattice Boltzmann method for multi-component fluids with near-contact interactions [28, 29] which reproduce the experimental findings. The simulations employ a perfectly monodisperse emulsion which demonstrates that the observed stochasticity of the system is intimately associated with the granular structure and not, in particular, with polydispersity of the droplets.

The droplets ('grains') of the innermost phase are reproducibly formed at a T-junction of channels of rectangular cross-sections. Subsequently, the monodisperse emulsion is pushed into a wider channel (see Fig. 1) and focused by the continuous phase into an orifice. We use three Newtonian liquids to formulate the double emulsion: fluorinated fluid [30] as the continuous phase, oil with surfactant as the middle (lubricating) phase, and dyed water as the innermost 'grain' phase (see SM for details). The T-junction generates droplets at a volume fraction of 86% (the highest possible for which the emulsion is monodisperse and stable). Based on measured frequency of generation of the aqueous droplets, we estimate droplet volume to be around 0.11 pL which yields the diameter of an undeformed spherical droplet $D_0 = 0.28$ mm. Since the value of D_0 is larger than the channel height $H = 0.11$ mm, the droplets are flattened by the lower and upper walls. Based on the measured apparent areas of the generated clusters we estimate the diameter of the flattened droplets $D_{||} = 0.37$ mm with a coefficient of variation $CV_{D_{||}} = 9.2\%$.

The ensuing emulsion is stable enough to produce flows for several minutes, with only occasional coalescence of the aqueous droplets.

Our LB simulations, performed using a fully three-dimensional Color-Gradient approach augmented with near-contact interactions [28, 29], use slightly different, but similar, parameters for the system and droplets. See SM and [31] for details on the simulation methods and implementation.

In the experiment, we change the flow rate of the continuous phase Q_c , while keeping the flow rate of the dispersed phase (the emulsion) Q_d constant and equal $Q_d = 0.5$ mL/h [32]. As a result, we observe several types of dynamic flow patterns as illustrated in Fig. 2 and movies SM1-SM4. We find superficial similarity to jetting and dripping regimes present in simple fluids, however

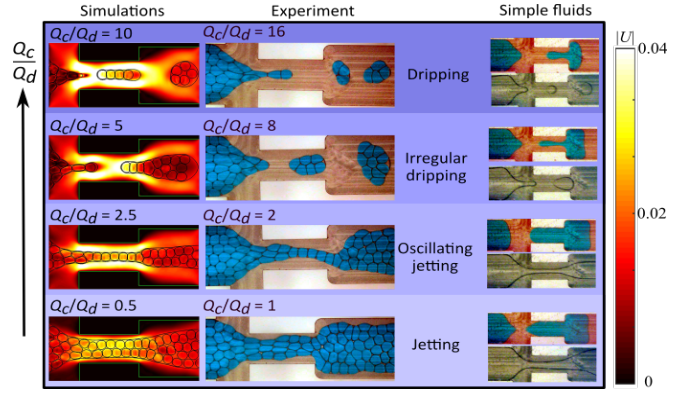


FIG. 2. Dynamical modes observed in the system upon varying Q_c/Q_d $Q_d = 0.5$ mL/h. Q_c/Q_d decreases from top to bottom (note different values for simulations and experiment). Smaller snapshots in the column on the right show flow patterns observed in the experiment with the emulsion replaced by a simple viscous liquid, either water (blue) or oil (transparent) for the same Q_c/Q_d as in the experiment with the emulsion. The colorbar refers to simulation snapshots, with U being the local velocity in lattice units. Experimental snapshots were taken from movies SM1 ($Q_c/Q_d = 1$), SM2 ($Q_c/Q_d = 2$), SM3 ($Q_c/Q_d = 8$), SM 4 ($Q_c/Q_d = 16$); simulation-based snapshots are taken from movies SM5 ($Q_c/Q_d = 0.5$), SM6 ($Q_c/Q_d = 2.5$), SM7 ($Q_c/Q_d = 5$), SM8 ($Q_c/Q_d = 10$)

the observed dynamics is much richer. We can distinguish four different modes: (i) jetting with a large and moderately oscillating jet width, further referred to simply as *jetting* (ii) jetting with thin, strongly oscillating jets and occasional break-up, further referred to as *oscillating jetting* (iii) dripping resulting in a strongly polydisperse double-emulsion, further referred to as *irregular dripping* (iv) dripping resulting in a relatively monodisperse double-emulsion, further referred to simply as *dripping*. The numerical simulations recreate the same dynamical modes at values Q_c/Q_d similar to yet slightly different than the experimental ones, see Fig. 2 and movies SM5-SM8. We attribute the differences to slightly different geometrical parameters and volume fractions as imposed by the numerical constraints (see SM).

In order to understand the impact of granularity of the focused fluid on the onset of *oscillating jetting/irregular dripping* regimes, we repeat the flow focusing experiment with a simple fluid (water or oil) as the dispersed phase. We find simple jetting (see SM9 and SM10 for oil at $Q_c/Q_d = 1$ and 2 respectively), highly monodisperse dripping ($CV_{A_{||}} = 2.2\%$ for oil, where $A_{||}$ is the area of a flattened oil drop, at $Q_c/Q_d = 3$; see SM11) or bi-disperse dripping [33] (the latter, with 2 narrow peaks, in the case with oil at high Q_c/Q_d , see SM12 and SM13 for examples with $Q_c/Q_d = 4$ and 8 respectively); see SM for relevant histograms), but never observe irregular oscillations and rich dynamics similar to the case of a focused emulsion (see Fig. 2). In particular, we find only dripping for the case with water and the jetting-dripping transition for oil, which both agree with previous predic-

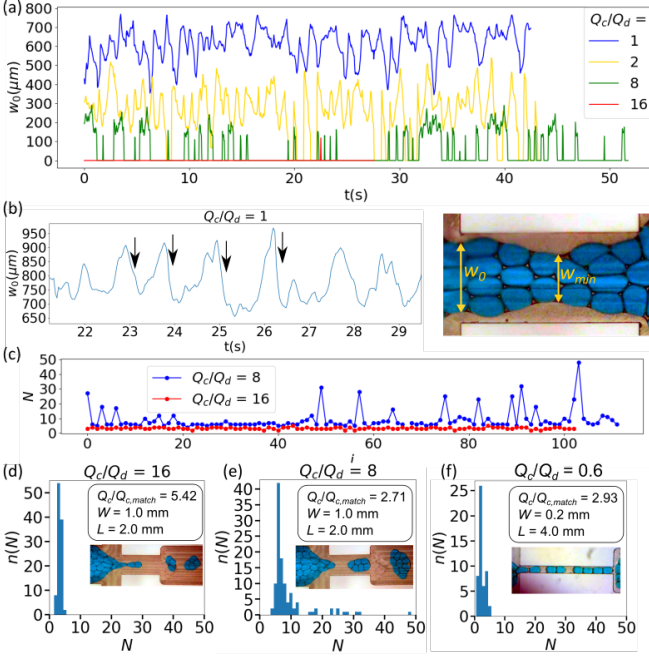


FIG. 3. (a) Fluctuations of the minimum jet width $w_{min}(t)$ (b) Fluctuations of jet width $w_0(t)$ at the entrance to the constriction. The avalanche-like events are marked with arrows. (c) Number of grains N in clusters generated in the *dripping* and *irregular dripping* regimes ($Q_c/Q_d = 16$ and 8) vs the index of cluster i in order of generation, and (d)-(e) the corresponding histograms $n(N)$. The histogram in (f) shows analogous data for a system with a much thinner and longer orifice, yet with $Q_c/Q_{c,match}$ very close to the case in (e) (see main text and SM for further discussion).

tions for simple Newtonian liquids (i.e., that increasing viscosity of the dispersed phase promotes jetting) [26].

We further examine the four distinct dynamical modes observed for the focused emulsion in more detail. We define the minimum instantaneous jet width, $w_{min}(t) = \min_{x \in [0, L]} w(x, t)$ where $w(x, t)$ is the full spatio-temporal profile of the jet within the narrowing, as a measure of jet oscillations in time (Fig. 3a). We find that the corresponding time average, $\langle w_{min} \rangle = T^{-1} \int_0^T dt w_{min}(t)$, where T is the time of duration of the experiment, decreases upon increasing Q_d/Q_c while the stochastic fluctuations of $w_{min}(t)$ remain of similar absolute magnitude. Accordingly, this leads to occasional break-up ($w_{min} = 0$) of the jet in the oscillating jetting mode.

Additionally, in the *jetting* mode, we frequently observe abrupt granular ‘discharge’ of the junction, associated with rapid entrance of several droplets in-parallel into the constriction. In order to quantify such avalanche-like behavior we measure the width of the jet $w_0(t)$ precisely at the entrance to the constriction. We find that $w_0(t)$ develops a saw-tooth like profile (Fig. 3b) characteristic of avalanches and previously also observed in sheared foams and dense suspensions [12, 34].

Next, we measure the sizes of the subsequently gen-

erated clusters in the *dripping* and *irregular dripping* modes (Fig. 3c). Whereas in the former case the clusters are relatively monodisperse (yet much more polydisperse than in dripping of simple viscous fluids), in the latter case we observe recurring peaks in the cluster size corresponding to extremely large clusters. More quantitatively, in the *dripping* mode the number of grains N in a cluster does not apparently deviate from the Gaussian distribution. The coefficient of variation $CV_N = 19.5\%$ (see Fig. 3d) is significantly larger than in the case with the granular emulsion replaced by the pure oil phase ($CV_{A_{||}} = 2.2\%$), yet still moderate. In contrast, in the *irregular dripping* mode the distribution of cluster sizes N features a long right tail for large N (see Fig. 3e), with $CV_N = 74.3\%$ and a very large skewness, as documented by a Pearson’s moment coefficient of skewness (see SM for a formal definition) $S_N = 3.1$.

We associate the formation of the extremely large clusters in the irregular dripping regime with the emergence of single-file chains of grains within the narrowing, which, once formed, exhibit remarkable stability. In principle, such chains remain stable once the local velocity of the continuous phase around the chain U_c matches the velocity of the grains inside the chain $U_{d,chain}$, which in turn is set by the rate of feeding of the grains into the orifice (note that this condition also determines the boundary between the dripping and jetting modes). Considering that $U_c = Q_c/[H \times (W - W_{chain})]$ and $U_{d,chain} = Q_d/(H \times W_{chain})$, where W_{chain} is the width of the chain, the requirement $U_c = U_{d,chain}$ leads to the following condition on the matching flow rate of the continuous fluid $Q_{c,match}$:

$$Q_{c,match}/Q_d = W/W_{chain} - 1 \quad (1)$$

We note that this requirement resembles the condition for continuity of soft polymer fibers stretched by an accelerating co-flow, studied by Mercader et al. [35]. In fact, our granular chains resemble semi-solid fibers rather than viscous jets as demonstrated by (i) the lack of the Rayleigh-Plateau instability (typical of viscous jets) [25] and (ii) longitudinal stretching and/or compression of the chain as visualized by droplet deformations within the constriction, see Fig. 4a. We associate such elastic solid-like behavior with a combination of the capillary arrest and deformability of the droplets within the chain.

From the experimentally measured average width of chain $W_{chain} = 0.68D_{||} = 0.253W$ we obtain $Q_{c,match}/Q_d = 2.95$. This is close to the value $Q_c/Q_d = 2$ corresponding to the *oscillating jetting* regime; however, we actually observe single-file chains more often when $Q_c/Q_d = 8$, in the *irregular dripping* mode. We suspect that the relative scarcity of single-file chains for $Q_c/Q_d = 2$ results from spontaneous ‘folding’ of single-file chains into wider jets in the immediate vicinity of the theoretical matching velocity $U_{d,chain}$ (see SM2, frames 51-72, 145-164, 670-691). At the same time, due to the finite length of the orifice L , chains are able to survive

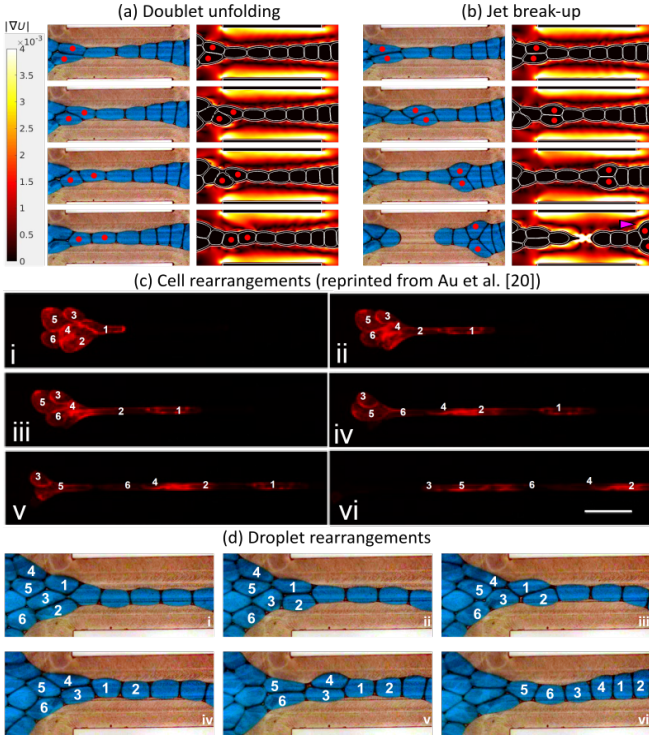


FIG. 4. (a)-(b) Numerical (at $Q_c/Q_d = 3.5$) and experimental (at $Q_c/Q_d = 8$) snapshots (see SM14 and SM15 respectively for the full movies) visualizing (a) doublet unfolding upon entry into the constriction and (b) a failure of unfolding, leading to an increased velocity gradient ∇U around the doublet (pink marker in the simulation panel) and break-up of the jet. (c) The order of entry of cells forming a CTC cluster in a narrowing channel under co-flow (figure adapted with permission from Au et al. [20]; copyright National Academy of Sciences 2016) and (d) the order of entry of droplets into the constriction in our experiment, at $Q_c/Q_d = 8$ (see SM16 for the full movie).

extensional stresses at $Q_c \gtrsim Q_{c,match}$ which may explain their abundance at $Q_c/Q_d = 8$.

We note that even at matched velocities the chains can break due to irregularity of the grain feeding into the orifice associated with stochasticity of grain rearrangements upon approaching the constriction. When a pair of grains enter the narrowing simultaneously they may rearrange, or ‘unfold’, into a chain or not- in the latter case entering as a 2-grain cluster or a ‘fold’ (see Fig. 4). When the fold enters the orifice the continuous phase needs to locally accelerate and pass around it to conserve flux. The increased viscous forces acting at the fold result in chain stretching via longitudinal grain deformation which may eventually cause chain breakup.

Our LB simulations allow us to extract precise information about the velocity gradients within the system and verify this scenario. Indeed, we find progressively increasing velocity gradients around the doublet (see the purple marker in the last snapshot of Fig. 4b). We propose that a similar mechanism (i.e., the acceleration of

the continuous phase around wider parts of the jet) might also lead to the enhancement of fluctuations of jet width in the *jetting* and the *oscillating jetting* modes.

Next, we also perform a series of experiments with a smaller width of the orifice ($W \lesssim D_{||}$), for which a simultaneous entry of two grains into the narrowing is hindered (see SM for details). In this case, the complex dynamical picture is lost and we only observe a transition between single-file jetting and dripping. To provide an example, we quantify the cluster size distribution in this geometry in Fig. 3f when $Q_c/Q_{c,match}$ (which serves as a measure of proximity to the jetting-dripping transition) is almost identical as in the long-tailed *irregular dripping* mode (Fig. 3e). We still observe strong polydispersity ($CV_N = 44\%$), however, no long tails ($S_N = 0.73$). This further confirms the impact of individual grain rearrangements and, more specifically, the manner in which the grains enter the constriction, on the fate of the entire system, including the large-scale stochastic behavior.

Finally, we provide an example of how granular rearrangements observed in our flow-focusing setup could serve as a ‘benchmark’ for more complex soft granular flows including confined biological flows. In fact, sequences of cell rearrangements have been previously studied in circulating tumor cell clusters transiting a narrowing channel [20]. Upon approaching a constriction the clusters were often able to unfold into a single-file chain without break-up. In some cases, the order in which the cells approached the narrowing seemed to determine their order of entry, but in some other cases the order was strongly disturbed by cell rearrangements (see Fig. 4c). This is interpreted in [20] as the effect of heterogeneity of cell-cell interactions and polydispersity of cells. However, our experiments demonstrate that even in a homogeneous, monodisperse *passive* granular system the order of entry is not strictly determined by the order of approach but rather depends on stochastic rearrangements upon entry (see Fig. 4d). Accordingly, we argue that the phenomena reported by Au et al. [20] may result from the immanent irregularity of flow patterns associated with many-body interactions and general stochastic dynamics of soft granular media, and not only from heterogeneity of the grains.

In summary, we develop a model platform to study the behaviour of soft granular media subjected to external flows and demonstrate rich phenomenology including stochastic granular jetting- and dripping-like modes with no counterpart in simple fluids.

We note that series of two (or more) microfluidic junctions have been previously used to produce double-emulsion core-shell droplets with multiple cores [36–42]. A couple of recent works considered cores-in-shell volume fractions high enough ($> 80\%$) for the double-emulsion drops to be considered soft granular clusters. [17, 37, 43, 44]. However, those previous works exploited generation of the clusters via one-by-one feeding of the cores into the shell without actually considering the flow of a soft-granular medium *per se*. In this Letter, we ar-

gue that the latter poses a completely different problem and involves phenomena not present in simple fluids.

Our findings open up several avenues for future work. First, the full dynamical phase diagram in the 3-dimensional (Q_c, Q_d, ϕ) -space including possible hysteretic behavior at transitions between the modes—also depending on the viscosities and interfacial tensions—remains to be established. Second, the statistics of rearrangements between individual grains could be further investigated to shed light on the effective phases of matter (solid- vs fluid-like) occurring in such a system. Finally, our platform could also be further developed to allow tracking of the internal relaxation dynamics of the generated granular clusters. This poses possible significance e.g., to the recovery of tissues after mechanical injury or the dynamics of CTC's in capillaries during cancer metastasis.

The authors acknowledge funding from the Euro-

pean Research Council under the European Union's Horizon 2020 Framework Programme (Grant No. FP/2014–2020), ERC Grant Agreement No. 739964 (COPMAT), Marie Skłodowska-Curie grant No. 847413 and the PRACE 16DECI0017 RADOBI project. M.B. acknowledges the PMW programme of the Minister of Science and Higher Education in the years 2020–2024 no. 5005/H2020-MSCA-COFUND/2019/2. A.M. acknowledges the CINECA Computational Grant ISCRA-C IsC83 - “SDROMOL”, id. HP10CZXK6R under the ISCRA initiative, for the availability of high performance computing resources needed to run the simulations and the support provided. J.G. acknowledges support from Foundation for Polish Science within First Team program under grant no POIR.04.04.00-00-26C7/16-00. The authors thank PRL reviewers for insightful comments which helped to significantly improve the quality of the manuscript. M.B. and J.G. thank Patryk Adamczuk and Mikołaj Boroński for technical assistance.

-
- [1] K. Guevorkian, M. J. Colbert, M. Durth, S. Dufour, and F. Brochard-Wyart, Aspiration of biological viscoelastic drops, *Physical Review Letters* **104**, 1 (2010), arXiv:1003.4372.
 - [2] S. Douezan, K. Guevorkian, R. Naouar, S. Dufour, D. Cuvelier, and F. Brochard-Wyart, Spreading dynamics and wetting transition of cellular aggregates., *Proceedings of the National Academy of Sciences of the United States of America* **108**, 7315 (2011).
 - [3] M. L. Manning, R. A. Foty, M. S. Steinberg, and E.-M. Schoetz, Coaction of intercellular adhesion and cortical tension specifies tissue surface tension, *Proceedings of the National Academy of Sciences* **107**, 12517 (2010), arXiv:77955440431.
 - [4] S. Cohen-Addad, R. Höhler, and O. Pitois, Flow in foams and flowing foams, *Annual Review of Fluid Mechanics* **45**, 241 (2013).
 - [5] S. Nezamabadi, T. H. Nguyen, J. Y. Delenne, and F. Radjai, Modeling soft granular materials, *Granular Matter* **19**, 1 (2017).
 - [6] A. A. J. Kabla, Collective cell migration: leadership, invasion and segregation., *Journal of the Royal Society Interface* **9**, 3268 (2012), arXiv:arXiv:1108.4286v1.
 - [7] S. Pawlizak, A. W. Fritsch, S. Grosser, D. Ahrens, T. Thalheim, S. Riedel, T. R. Kiessling, L. Oswald, M. Zink, M. L. Manning, and J. A. Käs, Testing the differential adhesion hypothesis across the epithelial-mesenchymal transition, *New Journal of Physics* **17**, 83049 (2015).
 - [8] Y. Gai, C. M. Leong, W. Cai, and S. K. Tang, Spatiotemporal periodicity of dislocation dynamics in a two-dimensional microfluidic crystal flowing in a tapered channel, *Proceedings of the National Academy of Sciences of the United States of America* **113**, 12082 (2016).
 - [9] Y. Gai, J. W. Khor, and S. K. Tang, Confinement and viscosity ratio effect on droplet break-up in a concentrated emulsion flowing through a narrow constriction, *Lab on a Chip* **16**, 3058 (2016).
 - [10] Y. Jiang, P. J. Swart, A. Saxena, M. Asipauskas, and J. A. Glazier, Hysteresis and avalanches in two-dimensional foam rheology simulations, *Physical Review E - Statistical Physics, Plasmas, Fluids, and Related Interdisciplinary Topics* **59**, 5819 (1999).
 - [11] P. Marmottant and F. Graner, Plastic and viscous dissipations in foams: Cross-over from low to high shear rates, *Soft Matter* **9**, 9602 (2013).
 - [12] P. Kumar, E. Korkolis, R. Benzi, D. Denisov, A. Niemeijer, P. Schall, F. Toschi, and J. Trampert, On interevent time distributions of avalanche dynamics, *Scientific Reports* **10**, 1 (2020).
 - [13] J. Goyon, A. Colin, G. Ovarlez, A. Ajdari, and L. Bocquet, Spatial cooperativity in soft glassy flows, *Nature* **454**, 84 (2008).
 - [14] J. Goyon, A. Colin, and L. Bocquet, How does a soft glassy material flow: finite size effects, non local rheology, and flow cooperativity, *Soft Matter* **6**, 2668 (2010).
 - [15] M. Lulli, R. Benzi, and M. Sbragaglia, Metastability at the Yield-Stress Transition in Soft Glasses, *Physical Review X* **8**, 21031 (2018), arXiv:1710.00686.
 - [16] M. D. Uchic, D. M. Dimiduk, J. N. Florando, and W. D. Nix, Sample dimensions influence strength and crystal plasticity, *Science* **305**, 986 (2004).
 - [17] M. Constantini, J. Guzowski, P. J. Żuk, P. Mozetic, S. De Panfilis, J. Jaroszewicz, M. Heljak, M. Massimi, M. Pierron, M. Trombetta, M. Dentini, W. Świąszkowski, A. Rainer, P. Garstecki, and A. Barbetta, Electric Field Assisted Microfluidic Platform for Generation of Tailorable Porous Microbeads as Cell Carriers for Tissue Engineering, *Advanced Functional Materials* **28**, 1 (2018).
 - [18] M. Constantini, J. Jaroszewicz, Ł. Kozioł, K. Szlązak, W. Świąszkowski, P. Garstecki, C. Stubenrauch, A. Barbetta, and J. Guzowski, 3D Printing of Functionally Graded Porous Materials Using On-Demand Reconfigurable Microfluidics, *Angewandte Chemie* **131**, 7702 (2019).
 - [19] C. B. Highley, K. H. Song, A. C. Daly, and J. A. Burdick, Jammed Microgel Inks for 3D Printing Applications, *Ad-*

- vanced Science **6**, 10.1002/advs.201801076 (2019).
- [20] S. H. Au, B. D. Storey, J. C. Moore, Q. Tang, Y. L. Chen, S. Javaid, A. F. Sarioglu, R. Sullivan, M. W. Madden, R. O’Keefe, D. A. Haber, S. Maheswaran, D. M. Lange-
nau, S. L. Stott, and M. Toner, Clusters of circulating
tumor cells traverse capillary-sized vessels, *Proceedings
of the National Academy of Sciences of the United States
of America* **113**, 4947 (2016).
 - [21] J. P. Raven and P. Marmottant, Microfluidic crystals:
Dynamic interplay between rearrangement waves and
flow, *Physical Review Letters* **102**, 1 (2009).
 - [22] P. Garstecki and G. M. Whitesides, Flowing crystals:
Nonequilibrium structure of foam, *Physical Review Let-
ters* **97**, 1 (2006).
 - [23] S. L. Anna, N. Bontoux, and H. A. Stone, Formation of
dispersions using ”flow focusing” in microchannels, *Ap-
plied Physics Letters* **82**, 364 (2003).
 - [24] C. N. Baroud, F. Gallaire, and R. Danga, Dynamics of
microfluidic droplets, *Lab on a Chip* **10**, 2032 (2010).
 - [25] A. S. Utada, A. Fernandez-Nieves, H. A. Stone, and D. A.
Weitz, Dripping to jetting transitions in coflowing liquid
streams, *Physical Review Letters* **99**, 1 (2007).
 - [26] T. Cubaud and T. G. Mason, Capillary threads and vis-
cous droplets in square microchannels, *Physics of Fluids*
20 (2008).
 - [27] N. M. Kovalchuk, M. Sagisaka, K. Steponavicius,
D. Vigolo, and M. J. Simmons, Drop formation in mi-
crofluidic cross-junction: jetting to dripping to jetting
transition, *Microfluidics and Nanofluidics* **23**, 1 (2019).
 - [28] A. Montessori, M. Lauricella, N. Tirelli, and S. Succi,
Mesoscale modelling of near-contact interactions for com-
plex flowing interfaces, *Journal of Fluid Mechanics* **872**,
327 (2019).
 - [29] A. Montessori, M. Lauricella, and A. Tiribocchi, Mod-
eling pattern formation in soft flowing crystals, *Physical
Review Fluids* **4**, 72201 (2019).
 - [30] C. Holtze, A. C. Rowat, J. J. Agresti, J. B. Hutchison,
F. E. Angilè, C. H. Schmitz, S. Köster, H. Duan, K. J.
Humphry, R. A. Scanga, J. S. Johnson, D. Pisignano,
and D. A. Weitz, Biocompatible surfactants for water-in-
fluorocarbon emulsions, *Lab on a Chip* **8**, 1632 (2008).
 - [31] A. Montessori, A. Tiribocchi, M. Lauricella, F. Bonac-
corso, and S. Succi, Mesoscale modelling of droplets’ self-
assembly in microfluidic channels, *Soft Matter* **17**, 2374
(2021).
 - [32] At such Q_d the emulsion was possibly most stable.
 - [33] P. Garstecki, M. J. Fuerstman, and G. M. Whitesides,
Nonlinear dynamics of a flow-focusing bubble generator:
An inverted dripping faucet, *Physical Review Letters* **94**,
38 (2005).
 - [34] D. J. Durian, Foam mechanics at the bubble scale, *Phys-
ical Review Letters* **75**, 4780 (1995).
 - [35] C. Mercader, A. Lucas, A. Derré, C. Zakri, S. Moisan,
M. Maugey, and P. Poulin, Kinetics of fiber solidification,
*Proceedings of the National Academy of Sciences of the
United States of America* **107**, 18331 (2010).
 - [36] S. Okushima, T. Nisisako, T. Torii, and T. Higuchi, Con-
trolled production of monodisperse double emulsions by
two-step droplet breakup in microfluidic devices, *Lang-
muir* **20**, 9905 (2004).
 - [37] D. Lee and D. A. Weitz, Nonspherical colloidosomes with
multiple compartments from double emulsions, *Small* **5**,
1932 (2009).
 - [38] J. Wan, A. Bick, M. Sullivan, and H. A. Stone, Control-
lable microfluidic production of microbubbles in water-in-
oil emulsions and the formation of porous microparticles,
Advanced Materials **20**, 3314 (2008).
 - [39] A. R. Abate and D. A. Weitz, High-order multiple
emulsions formed in poly(dimethylsiloxane) microflu-
idics, *Small* **5**, 2030 (2009).
 - [40] L. L. Adams, T. E. Kodger, S. H. Kim, H. C. Shum,
T. Franke, and D. A. Weitz, Single step emulsification
for the generation of multi-component double emulsions,
Soft Matter **8**, 10719 (2012).
 - [41] A. S. Utada, E. Lorenceau, D. R. Link, P. D. Kaplan,
H. A. Stone, and D. A. Weitz, Monodisperse double
emulsions generated from a microcapillary device, *Sci-
ence* **308**, 537 (2005).
 - [42] G. T. Vladislavljević, R. Al Nuamani, and S. A. Nabavi,
Microfluidic production of multiple emulsions, *Microma-
chines* **8**, 10.3390/mi8030075 (2017).
 - [43] J. Guzowski and P. Garstecki, Droplet Clusters: Explor-
ing the Phase Space of Soft Mesoscale Atoms, *Physical
Review Letters* **114**, 1 (2015).
 - [44] S. H. Kim, H. Hwang, C. H. Lim, J. W. Shim, and S. M.
Yang, Packing of emulsion droplets: Structural and func-
tional motifs for multi-cored microcapsules, *Advanced
Functional Materials* **21**, 1608 (2011).

Supplemental Material for the article *Stochastic jetting and dripping in confined soft granular flows*

Michał Bogdan,^{1,*} Andrea Montessori,² Adriano Tiribocchi,³ Fabio Bonaccorso,^{3,4}

Marco Lauricella,³ Leon Jurkiewicz,¹ Sauro Succi,^{3,5,6} and Jan Guzowski^{1,†}

¹*Institute of Physical Chemistry, Polish Academy of Sciences, Kasprzaka 44/52, 01-224 Warsaw, Poland*

²*Dipartimento di Ingegneria, Università degli Studi Roma tre, via Vito Volterra 62, Rome, 00146, Italy*

³*Istituto per le Applicazioni del Calcolo del Consiglio Nazionale delle Ricerche, via dei Taurini 19, 00185, Rome, Italy*

⁴*Department of Physics and National Institute for Nuclear Physics,*

University of Rome "Tor Vergata", Via Cracovia, 50, 00133 Rome, Italy

⁵*Center for Life Nanoscience at la Sapienza, Istituto Italiano di Tecnologia, viale Regina Elena 295, 00161, Rome, Italy*

⁶*Department of Physics, Harvard University, 17 Oxford St, Cambridge, MA 02138, United States*

(Dated: January 26, 2022)

MATERIALS AND METHODS

All microfluidic channels are fabricated via milling in polycarbonate. Precise parameters of the Newtonian liquids used to formulate the double emulsion: fluorinated fluid FC40 with 1% w/w fluorosurfactant (PFPE-PEG-PFPE [30]) as the continuous phase, a mixture of silicone oil (PMX 200, 5cSt), hexadecane, and the surfactant SPAN80 in w/w proportions 70:30:1 as the middle (lubricating) phase (referred in the main text and further here as 'oil'), and water dyed with 0.1% w/w Erioglaucine as the innermost 'grain' phase. Based on literature values, we estimate the corresponding viscosities to be 4.1, 4.0, and 3.4 mPa s, respectively. The interfacial tensions of the water-oil and oil-external interfaces are 3.4 and 4.9 mN/m, respectively, as measured by pendant drop method.

In LB simulations, the geometrical parameters, expressed in simulation units, are as follows: $W_0 = L = 280$, $W = 140$, $H = 30$, while the total length of the computational domain is 846. The droplets are generated by imposing an internal boundary condition, as proposed in [31]; the volume fraction is estimated as ~ 0.75 , with a completely uniform droplet diameter of $D = 45$ simulation units.

FORMAL DEFINITION OF PEARSON'S COEFFICIENT OF SKEWNESS

The formal definition of the Pearson's moment coefficient of skewness S_X for a random variable X (which we use to quantitatively assess the asymmetry of the measured probability distributions of sizes of granular clusters) is: .

$$S_X = E \left[\left(\frac{X - \mu_X}{\sigma_X} \right)^3 \right] \quad (1)$$

Where E is the expectation value of the expression in the squared parenthesis, while μ_X and σ_X are respec-

tively the mean and standard deviation of the variable X .

EXPERIMENTS WITH ALTERNATIVE SYSTEM DIMENSIONS

In order to further verify the role of the formation of 2-grain 'folds' upon entry into the orifice in the behavior of the system, we repeat the experiments in an alternative set-up, in which the orifice is narrow enough to prevent the formation of such folds. The microfluidic system is again as in Fig. 1 of the main text, but with the following dimensions modified to the values specified: $W = 0.2$ mm, $L = 4$ mm, $H = 0.18$ mm. Note this means the orifice is now narrower than the diameter of a single grain. As expected, the simultaneous entry of two droplets into the narrowing is now impossible (see Fig. 1 and supporting movies, respectively SM17 for $Q_c/Q_d=0.4$, SM18 for $Q_c/Q_d=0.5$, SM19 for $Q_c/Q_d=0.6$, SM20 for $Q_c/Q_d=0.8$). The complex dynamical picture as described in the main text is now lost, with long right tails characteristic of the *irregular dripping* regime absent; we now observe a simple transition between jetting and dripping upon increasing Q_c/Q_d , with a reduction of cluster size within the dripping regime upon a further increase of Q_c/Q_d .

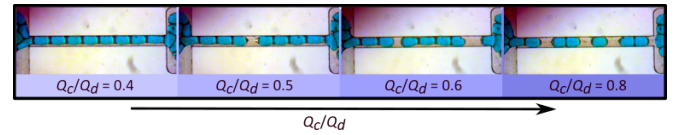


FIG. 1. Behavior of the emulsion upon passing a very narrow constriction under varying Q_c/Q_d .

FLOW FOCUSING OF PURE 'OIL'

In Fig. 2 we illustrate the effect of granularity on the variation of the areas of formed clusters/drops by com-

paring histograms of N for the emulsion's granular *dripping* mode (panel c) with histograms of $A_{||}$ for monodisperse (panel a) and bi-disperse (panel b) dripping modes of the oil itself. The x axes are re-normalised to the mean of the distribution in each case to help visualise relative variations.

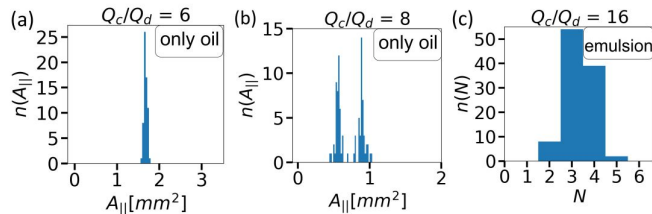


FIG. 2. Histograms of numbers of grains N in clusters of the emulsion $n(N)$ and of areas $A_{||}$ of flattened drops of the oil $n(A_{||})$, formed during dripping of the emulsion and the pure oil respectively.

* mbogdan@ichf.edu.pl

† jguzowski@ichf.edu.pl

- [1] K. Guevorkian, M. J. Colbert, M. Durth, S. Dufour, and F. Brochard-Wyart, Aspiration of biological viscoelastic drops, *Physical Review Letters* **104**, 1 (2010), arXiv:1003.4372.
- [2] S. Douezan, K. Guevorkian, R. Naouar, S. Dufour, D. Cuvelier, and F. Brochard-Wyart, Spreading dynamics and wetting transition of cellular aggregates., *Proceedings of the National Academy of Sciences of the United States of America* **108**, 7315 (2011).
- [3] M. L. Manning, R. A. Foty, M. S. Steinberg, and E.-M. Schoetz, Coaction of intercellular adhesion and cortical tension specifies tissue surface tension, *Proceedings of the National Academy of Sciences* **107**, 12517 (2010), arXiv:77955440431.
- [4] S. Cohen-Addad, R. Höhler, and O. Pitois, Flow in foams and flowing foams, *Annual Review of Fluid Mechanics* **45**, 241 (2013).
- [5] S. Nezamabadi, T. H. Nguyen, J. Y. Delenne, and F. Radjai, Modeling soft granular materials, *Granular Matter* **19**, 1 (2017).
- [6] A. A. J. Kabla, Collective cell migration: leadership, invasion and segregation., *Journal of the Royal Society Interface* **9**, 3268 (2012), arXiv:arXiv:1108.4286v1.
- [7] S. Pawlizak, A. W. Fritsch, S. Grosser, D. Ahrens, T. Thalheim, S. Riedel, T. R. Kiessling, L. Oswald, M. Zink, M. L. Manning, and J. A. Käs, Testing the differential adhesion hypothesis across the epithelial-mesenchymal transition, *New Journal of Physics* **17**, 83049 (2015).
- [8] Y. Gai, C. M. Leong, W. Cai, and S. K. Tang, Spatiotemporal periodicity of dislocation dynamics in a two-dimensional microfluidic crystal flowing in a tapered channel, *Proceedings of the National Academy of Sciences of the United States of America* **113**, 12082 (2016).
- [9] Y. Gai, J. W. Khor, and S. K. Tang, Confinement and viscosity ratio effect on droplet break-up in a concen-

- trated emulsion flowing through a narrow constriction, *Lab on a Chip* **16**, 3058 (2016).
- [10] Y. Jiang, P. J. Swart, A. Saxena, M. Asipauskas, and J. A. Glazier, Hysteresis and avalanches in two-dimensional foam rheology simulations, *Physical Review E - Statistical Physics, Plasmas, Fluids, and Related Interdisciplinary Topics* **59**, 5819 (1999).
- [11] P. Marmottant and F. Graner, Plastic and viscous dissipations in foams: Cross-over from low to high shear rates, *Soft Matter* **9**, 9602 (2013).
- [12] P. Kumar, E. Korkolis, R. Benzi, D. Denisov, A. Niemeijer, P. Schall, F. Toschi, and J. Trampert, On interevent time distributions of avalanche dynamics, *Scientific Reports* **10**, 1 (2020).
- [13] J. Goyon, A. Colin, G. Ovarlez, A. Ajdari, and L. Bocquet, Spatial cooperativity in soft glassy flows, *Nature* **454**, 84 (2008).
- [14] J. Goyon, A. Colin, and L. Bocquet, How does a soft glassy material flow: finite size effects, non local rheology, and flow cooperativity, *Soft Matter* **6**, 2668 (2010).
- [15] M. Lulli, R. Benzi, and M. Sbragaglia, Metastability at the Yield-Stress Transition in Soft Glasses, *Physical Review X* **8**, 21031 (2018), arXiv:1710.00686.
- [16] M. D. Uchic, D. M. Dimiduk, J. N. Florando, and W. D. Nix, Sample dimensions influence strength and crystal plasticity, *Science* **305**, 986 (2004).
- [17] M. Constantini, J. Guzowski, P. J. Żuk, P. Mozetic, S. De Panfilis, J. Jaroszewicz, M. Heljak, M. Massimi, M. Pierron, M. Trombetta, M. Dentini, W. Świążkowski, A. Rainer, P. Garstecki, and A. Barbetta, Electric Field Assisted Microfluidic Platform for Generation of Tailorable Porous Microbeads as Cell Carriers for Tissue Engineering, *Advanced Functional Materials* **28**, 1 (2018).
- [18] M. Constantini, J. Jaroszewicz, L. Kozon, K. Szlęzak, W. Świążkowski, P. Garstecki, C. Stubenrauch, A. Barbetta, and J. Guzowski, 3D Printing of Functionally Graded Porous Materials Using On-Demand Reconfigurable Microfluidics, *Angewandte Chemie* **131**, 7702 (2019).
- [19] C. B. Highley, K. H. Song, A. C. Daly, and J. A. Burdick, Jammed Microgel Inks for 3D Printing Applications, *Advanced Science* **6**, 10.1002/advs.201801076 (2019).
- [20] S. H. Au, B. D. Storey, J. C. Moore, Q. Tang, Y. L. Chen, S. Javadi, A. F. Sarioglu, R. Sullivan, M. W. Madden, R. O'Keefe, D. A. Haber, S. Maheswaran, D. M. Langeau, S. L. Stott, and M. Toner, Clusters of circulating tumor cells traverse capillary-sized vessels, *Proceedings of the National Academy of Sciences of the United States of America* **113**, 4947 (2016).
- [21] J. P. Raven and P. Marmottant, Microfluidic crystals: Dynamic interplay between rearrangement waves and flow, *Physical Review Letters* **102**, 1 (2009).
- [22] P. Garstecki and G. M. Whitesides, Flowing crystals: Nonequilibrium structure of foam, *Physical Review Letters* **97**, 1 (2006).
- [23] S. L. Anna, N. Bontoux, and H. A. Stone, Formation of dispersions using "flow focusing" in microchannels, *Applied Physics Letters* **82**, 364 (2003).
- [24] C. N. Baroud, F. Gallaire, and R. Danga, Dynamics of microfluidic droplets, *Lab on a Chip* **10**, 2032 (2010).
- [25] A. S. Utada, A. Fernandez-Nieves, H. A. Stone, and D. A. Weitz, Dripping to jetting transitions in coflowing liquid streams, *Physical Review Letters* **99**, 1 (2007).

- [26] T. Cubaud and T. G. Mason, Capillary threads and viscous droplets in square microchannels, *Physics of Fluids* **20** (2008).
- [27] N. M. Kovalchuk, M. Sagisaka, K. Steponavicius, D. Vigolo, and M. J. Simmons, Drop formation in microfluidic cross-junction: jetting to dripping to jetting transition, *Microfluidics and Nanofluidics* **23**, 1 (2019).
- [28] A. Montessori, M. Lauricella, N. Tirelli, and S. Succi, Mesoscale modelling of near-contact interactions for complex flowing interfaces, *Journal of Fluid Mechanics* **872**, 327 (2019).
- [29] A. Montessori, M. Lauricella, and A. Tiribocchi, Modeling pattern formation in soft flowing crystals, *Physical Review Fluids* **4**, 72201 (2019).
- [30] C. Holtze, A. C. Rowat, J. J. Agresti, J. B. Hutchison, F. E. Angilè, C. H. Schmitz, S. Köster, H. Duan, K. J. Humphry, R. A. Scanga, J. S. Johnson, D. Pisignano, and D. A. Weitz, Biocompatible surfactants for water-in-fluorocarbon emulsions, *Lab on a Chip* **8**, 1632 (2008).
- [31] A. Montessori, A. Tiribocchi, M. Lauricella, F. Bonaccorso, and S. Succi, Mesoscale modelling of droplets' self-assembly in microfluidic channels, *Soft Matter* **17**, 2374 (2021).
- [32] At such Q_d the emulsion was possibly most stable.
- [33] P. Garstecki, M. J. Fuerstman, and G. M. Whitesides, Nonlinear dynamics of a flow-focusing bubble generator: An inverted dripping faucet, *Physical Review Letters* **94**, 38 (2005).
- [34] D. J. Durian, Foam mechanics at the bubble scale, *Physical Review Letters* **75**, 4780 (1995).
- [35] C. Mercader, A. Lucas, A. Derré, C. Zakri, S. Moisan, M. Maugéy, and P. Poulin, Kinetics of fiber solidification, *Proceedings of the National Academy of Sciences of the United States of America* **107**, 18331 (2010).
- [36] S. Okushima, T. Nisisako, T. Torii, and T. Higuchi, Controlled production of monodisperse double emulsions by two-step droplet breakup in microfluidic devices, *Langmuir* **20**, 9905 (2004).
- [37] D. Lee and D. A. Weitz, Nonspherical colloidosomes with multiple compartments from double emulsions, *Small* **5**, 1932 (2009).
- [38] J. Wan, A. Bick, M. Sullivan, and H. A. Stone, Controllable microfluidic production of microbubbles in water-in-oil emulsions and the formation of porous microparticles, *Advanced Materials* **20**, 3314 (2008).
- [39] A. R. Abate and D. A. Weitz, High-order multiple emulsions formed in poly(dimethylsiloxane) microfluidics, *Small* **5**, 2030 (2009).
- [40] L. L. Adams, T. E. Kodger, S. H. Kim, H. C. Shum, T. Franke, and D. A. Weitz, Single step emulsification for the generation of multi-component double emulsions, *Soft Matter* **8**, 10719 (2012).
- [41] A. S. Utada, E. Lorenceau, D. R. Link, P. D. Kaplan, H. A. Stone, and D. A. Weitz, Monodisperse double emulsions generated from a microcapillary device, *Science* **308**, 537 (2005).
- [42] G. T. Vladislavljević, R. Al Nuamani, and S. A. Nabavi, Microfluidic production of multiple emulsions, *Micromachines* **8**, 10.3390/mi8030075 (2017).
- [43] J. Guzowski and P. Garstecki, Droplet Clusters: Exploring the Phase Space of Soft Mesoscale Atoms, *Physical Review Letters* **114**, 1 (2015).
- [44] S. H. Kim, H. Hwang, C. H. Lim, J. W. Shim, and S. M. Yang, Packing of emulsion droplets: Structural and functional motifs for multi-cored microcapsules, *Advanced Functional Materials* **21**, 1608 (2011).